

# Isoscaling and symmentropy in confined systems

C.O.Dorso<sup>1</sup>, P.A. Gimenez Molinelli<sup>1</sup> and J. Lopez<sup>2</sup>

<sup>1</sup> Departamento de Física, FCEN, Universidad de Buenos Aires, Núñez, Argentina

<sup>2</sup> University of Texas at El Paso, El Paso, Texas 79968, USA

February 27, 2009

**Abstract.** Isoscaling is studied using classical molecular dynamics simulations of the clustering of confined systems composed by  $(N, Z)$  equal to  $(40, 40)$  and  $(40, 56)$ , at different energies and densities. We show that as energy is increased the value of the isoscaling coefficient  $\alpha$  approaches steadily the one corresponding to the symmentropy term. We also show the effect an expansion has on isoscaling by allowing the confined systems to expand freely.

**PACS.** 24.10.Lx key1 – 02.70.Ns key2

## 1 Introduction

With the development of experimental advances that allow the study of nuclear reactions using radioactive isotopes, the study of the isotopic degree of freedom has received considerable attention [1–5]. Among the goals pursued with these studies one can mention, the understanding of charge equilibration in heavy ion reactions, and the role played by the isotope asymmetry terms of the equation of state of nuclear matter [4].

One of the main tools for the analysis of this observable is based on the study of isotope yields of central collisions of similar, but isotopically different, reactions [1, 5]. The ratio of isotope yields from reactions 1 and 2,  $R_{21}(N, Z)$ , has been found to depend exponentially on the isotope neutron number  $N$ , and proton number  $Z$ :

$$R_{21}(N, Z) = \frac{Y_2(N, Z)}{Y_1(N, Z)} = C e^{\alpha N + \beta Z}, \quad (1)$$

where  $C$ ,  $\alpha$  and  $\beta$  are fitting parameters. Equations of the form of (1) can be linked, under some approximations, to primary isotope yields produced by the disassembling of equilibrated systems in the framework of microcanonical and grand canonical ensembles [4], as well as to breakups in canonical [6] ensembles.

One of the main reasons for the interest on isoscaling is the connection between isoscaling and the symmetry energy term which has been proposed in different works [7] by analyzing, for example, the fragmentation process in the framework of the grand canonical ensemble. It is then proposed that:

$$\alpha \sim \frac{4C_{sym}}{T} \left[ \left( \frac{Z_1}{A_1} \right)^2 - \left( \frac{Z_2}{A_2} \right)^2 \right]. \quad (2)$$

In recent articles we have studied the behavior and properties of this observable using both classical and geometrical models. In [8] we found isoscaling in simulations of classical systems and in [9] we have shown, both analytically and numerically, that it can also be observed in the framework of the nuclear percolation model; an effect totally due to the probabilistic aspects of the problem. Along the same line of work, in [10] we studied the effect particle correlations have on the coefficients of 1, and in [11] we finally concluded that isoscaling can be expected for any disassembling system based solely on probabilistic aspects.

This sequence of interesting results lead us to believe that the isoscaling observed in nuclear fragmentation is due to a variety of factors, among which sampling probability and nuclear interactions play a substantial role. In this article we focus on the competition between probabilistic, nuclear and dynamic effects. Using classical molecular dynamics we will study isoscaling produced in systems with two different EOS and disassembling in confined and expanding environments.

In particular, we will use two parameterizations of the interaction potential [12] corresponding to equations of state with compressibility of  $250 \text{ MeV}$  and  $530 \text{ MeV}$  to study equilibrated systems clustering in a spherical container as well as in a free expansion. To relate the isoscaling parameters directly to the EOS, we have calculated the symmetry energy terms of the droplet model for the two potentials used, and studied their effect on the evolutions of confined and expanding systems.

In section 2 we introduce the classical model used, describe how the symmetry energy terms were obtained for each of the parameterizations of the potential, and obtain their caloric curves. In section 3 we review the concept of symmentropy and study the isoscaling of confined and ex-

panding systems. The manuscript closes with a summary of the main conclusions.

## 2 Equations of state

Here the molecular dynamics model used for this study is introduced along with the two potentials corresponding to different compressibility, and the symmetry energy terms and caloric curves are obtained for each of these parameterizations of the potential.

### 2.1 Molecular dynamics model

To study the origin of isoscaling, a model capable of reproducing both the out-of-equilibrium and the equilibrium parts of a collision is highly desirable; in the present work, we use a molecular dynamics (*MD*) model that can describe non-equilibrium dynamics, hydrodynamic flow and changes of phase without adjustable parameters. The combination of this *MD* code with a fragment-recognition algorithm has been applied in recent years to study, among other phenomena, neck fragmentation [13], phase transitions [14], and other features of nuclear reactions, including isoscaling [15, 8].

The *MD* code uses a two-body potential composed of the Coulomb interaction plus a nuclear part [12] that correctly reproduces nucleon-nucleon cross sections, as well as the correct binding energies and densities of real nuclei. The “nuclear” part of the interaction potential is

$$V_{np}(r) = \begin{aligned} & V_r [\exp(-\mu_r r)/r - \exp(-\mu_r r_c)/r_c] \\ & - V_a [\exp(-\mu_a r)/r - \exp(-\mu_a r_a)/r_a] \end{aligned}$$

$$V_{nn}(r) = V_{pp}(r) = V_0 [\exp(-\mu_0 r)/r - \exp(-\mu_0 r_c)/r_c]$$

where the cutoff radius is  $r_c = 5.4 \text{ fm}$ ,  $V_{np}$  is the potential between a neutron and a proton while  $V_{nn}$  is that between identical nucleons. The values of the parameters of the Yukawa potentials [12] correspond to an equation of state of infinite nuclear matter with an equilibrium density of  $\rho_0 = 0.16 \text{ fm}^{-3}$ , a binding energy  $E(\rho_0) = -16 \text{ MeV/nucleon}$ , and a compressibility of  $\sim 250 \text{ MeV}$  for the medium model, and a compressibility of about  $535 \text{ MeV}$  for the stiff model.

### 2.2 Symmetry energy coefficients

To determine the coefficients of the droplet model corresponding to each set of the parameters of the potentials, we have used dissipative molecular dynamics to construct “nuclei” in their ground states. In a nutshell, individual nuclei were evolved and cooled until the proper values of the nuclear radius and binding energy were achieved. Taking such state as the ground state (still with some residual motion, which mimics Fermi motion) we proceeded to fit the resulting nuclei with

$$E/A = a_v + a_s * A^{-1/3} + a_c * (Z(Z-1)) * A^{-4/3} + 4a_{sym}(N-Z)^2 A^{-2},$$

**Table 1.** Comparison of coefficients obtained for different models

Coefficient	Stiff	Medium	Experimental
$a_v$	16.1	17.37	15.75
$a_s$	-11.73	-14.38	-17.8
$a_c$	-0.79	-0.9	-0.711
$a_{sym}$	-34.07	-25.08	-23.7

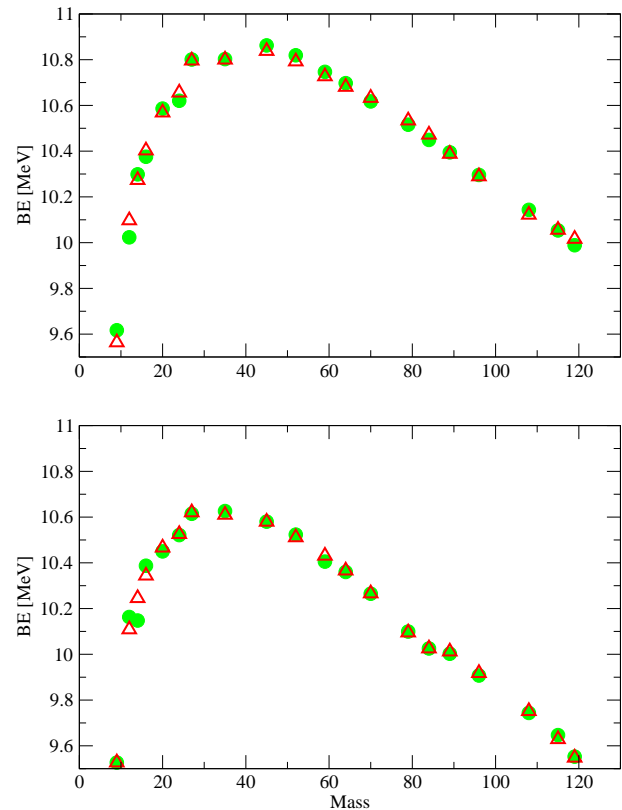


**Fig. 1.** Energies obtained with the mass formula fit (triangles) for the Stiff and Medium models (top and bottom panels respectively) together with the corresponding ground states calculated using frictional molecular dynamics (circles)

thus obtaining the values of the coefficients presented in Table1

Where, for comparison, we are also listing experimental data from the book of Rohlff [16].

In Fig. 1 we show the numerically obtained binding energies for the case of the Medium-model together with the corresponding fit.

Having calculated the symmetry energy coefficients for both parameterizations of the Illinois potential we are now able to use these potentials in order to explore the possibility of detecting the differences in symmetry energy using the isoscaling observable. As in previous works we

have analyzed, among others, the collisions of  $^{40}\text{Ca}+^{40}\text{Ca}$ ,  $^{48}\text{Ca}+^{48}\text{Ca}$  and  $^{56}\text{Ca}+^{56}\text{Ca}$  at different energies, in this study we linked to those analyses and study the evolution of constrained “nuclei” composed of  $(N, Z) = (40, 40)$  and  $(56, 40)$  corresponding to the total mass of the colliding partners in our previous works.

As done above we have used the dissipative molecular dynamics method to build nuclei in their ground states. Once the ground states are available, we place the resulting cold systems inside a spherical container. The radii of the container is fixed in order to obtain selected values of the number density ranging from 0.001 to 0.007. The different values of the energy are obtained by scaling the momenta of the particles. The trajectories of motion of individual nucleons are then calculated using the standard Verlet algorithm with an energy conservation of  $\mathcal{O}(0.01\%)$ . We first perform a long run in order to let the system relax to equilibrium. Afterwards a much longer run is performed and well separated in time snapshots of the evolution are recorded.

From the microscopic information of the evolution, given by the values of  $(\vec{r}, \vec{p})$  of the nucleons, we calculate the fragment structure of the system by means of a cluster-detection algorithm which, in this case, is the *MSTE* method which was introduced decades ago [17], but was recently adapted for this field, fully analyzed and compared with other fragment recognition algorithms [18]. According to this prescription, a particle  $i$  belongs to a cluster  $C$  if there is a particle  $j$  in  $C$  to which  $i$  is bound in the sense of  $p_{ij}^2/4\mu < v_{ij}$ , where  $p_{ij}$  is the magnitude of the relative momentum,  $\mu$  the reduced mass, and  $v_{ij}$  the interparticle potential. In this cluster definition the effect of the relative momentum between the particles that form the cluster is taken into account in an approximate way. It should be kept in mind that these clusters correspond to a given snapshot of the evolution. They are not stable in the sense that their lifetime is a function of the particle-particle collision frequency in the system.

The systems  $[N, Z](40, 40)$  and  $(56, 40)$ , were studied at different energies in the range  $-5$  to  $8$   $MeV/A$  and for four values of the number density with two thousand snapshots recorded at each energy.

Before we turn to a description of the analysis performed on these evolutions, a word of caution is needed to underline the fact that the *MD* model here described is fully classical, and that all quantal effects, such as the exclusion principle, Fermi motion and isotopic content-modifying phenomena, are excluded. [The effects of Fermi motion, although formally absent, are somewhat included by the internal motion of the “nucleons” in their “ground state” as explained before.] Therefore, any observed variations to isoscaling will be entirely due to the effect of the change of *EOS* and or to the effect of confinement.

## 2.3 Temperatures

We first calculated the kinetic temperatures given by

$$T_{kin} = \frac{2}{3} \frac{1}{N} \sum_{i=1}^N \frac{p_i^2}{2m} \quad (3)$$

with  $p_i$  representing the momentum of particle  $i$ , and  $N$  the total number of particles in the system. The corresponding caloric curves, defined as the functional relationship between the temperature of the system and its energy, are displayed in Fig. 2. It is interesting to notice that the systems displays the behavior already found in [19,20] for Lennard Jones systems, i.e. as the density is lowered the caloric curves start to develop a “loop” which signals the presence of a negative specific heat. This behavior has been traced to the appearance of “surfaces” in the system, which has been associated with a first order phase transition.

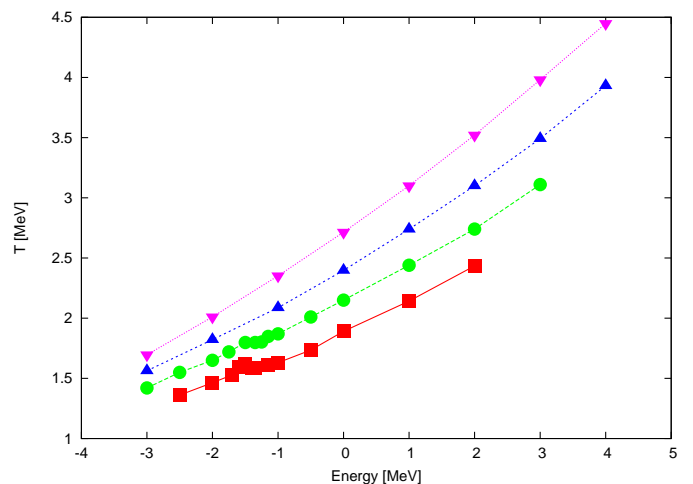


Fig. 2. Caloric curves for the medium model

## 3 Isoscaling

In this section we first briefly review the concept of symmentropy, recently introduced in [11] and afterwards we analyze the isoscaling properties of both confined and expanding systems described by the Illinois potential in its two parameterizations.

### 3.1 Symmentropy

It has been shown [10] that a good isoscaling signature appears even when there is no interaction at all and fragments are defined via a simple bond percolation approach.

Considering a square  $D$ -dimensional lattice with nodes occupied by “particles” of  $N$  colors. The total number of nodes is  $A$  and  $A = N + Z + R + \dots$  with  $N, Z, R, \dots$

denoting the number of nodes of given colors. Each color is assigned with a given probability  $p_Z, p_N, p_R$ , etc. with  $1 = p_Z + p_N + p_R + \dots$ . These probabilities are taken to be independent and homogeneous.

When working with two lattices differing in the relative content of the corresponding "colors" for the infinite case it is possible to derive the following relationship

$$R_{21}(N, Z, R, \dots) = \left[ \frac{p_{Z_2}}{p_{Z_1}} \right]^Z \left[ \frac{p_{N_2}}{p_{N_1}} \right]^N \left[ \frac{p_{R_2}}{p_{R_1}} \right]^R \dots = \exp(Z\beta + \alpha N + \delta R + \dots) \quad (4)$$

with

$$\beta = \ln \frac{p_{Z_2}}{p_{Z_1}} ; \alpha = \ln \frac{p_{N_2}}{p_{N_1}} ; \delta = \ln \frac{p_{R_2}}{p_{R_1}} ; \dots$$

For the finite case the following approximate expression is obtained

$$R_{21}(N, Z, R, \dots) = C \exp(Z\beta + \alpha N + \delta R + \dots) \quad (5)$$

with

$$C = \frac{p_{Z_1}}{p_{Z_2}} .$$

This relation reduces to the usual isoscaling expression when we consider two colors.

$$R_{21}(N, Z) = C \exp(\beta Z + \alpha N) \quad (6)$$

It is convenient to recall at this point the main assumptions used to obtain this result are a) the probabilities of color assignment to the nodes are independent, and b) the bond breaking probabilities are the same for the two lattices under consideration.

### 3.2 Isoscaling for confined systems

Data from the evolutions were used to construct the corresponding yield matrices  $Y_i(N, Z)$ , where  $i$  stands for the reaction, and  $N$  and  $Z$  for the neutron and proton numbers, respectively. These matrices were then used to calculate the ratio  $R_{21}(N, Z) = Y_2(N, Z)/Y_1(N, Z)$  for the combinations of the confined evolutions of the combined systems  $^{40}\text{Ca}+^{40}\text{Ca}$  with  $^{48}\text{Ca}+^{48}\text{Ca}$ . These ratios were calculated at the different conditions stated above. Fits to the isoscaling exponential law (1) were obtained using a standard least squares method for all points corresponding to each reaction and energy, procedure which yielded values of the parameters  $\alpha$  and  $\beta$  for each of the calculated times.

In what follows we will focus on the behavior of  $\alpha$  due to its importance after Eq. (2). In Fig. 3 we show this result for the medium model.

In Fig. 3 it is important to notice that  $\alpha$  is a decreasing function of the energy of the system, but more important, it converges to a constant value. This asymptotic value is quite close to the one corresponding to the symmentropy limit which states that

$$\alpha_S = \ln \left[ \frac{q_2}{q_1} \right] , \quad (7)$$

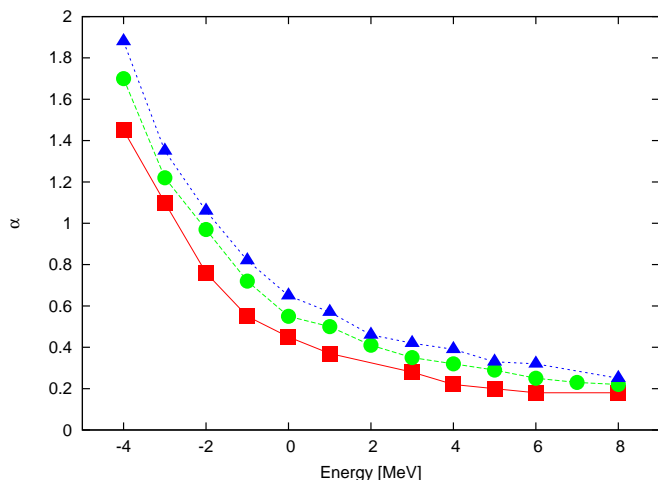


Fig. 3. Values of isoscaling coefficient  $\alpha$  for the medium model

with  $q_i$  given by the quotient  $N_i/A_i$ ; this suggests that in the limit of high energies the isoscaling behavior is dominated by the symmentropy term.

It is now interesting to find out to which extent this convergence to the probabilistic limit "blurs" the possibility of exploring the value of the symmetry energy term given by the two parameterizations of the potential. For this purpose we have fixed the number density of our confined systems in  $N/V = 0.007 \text{ fm}^{-3}$  and performed the same calculations for both potentials. As before we calculate the value of  $\alpha$  for each case and then we plot them together. This is displayed in Fig. 4.

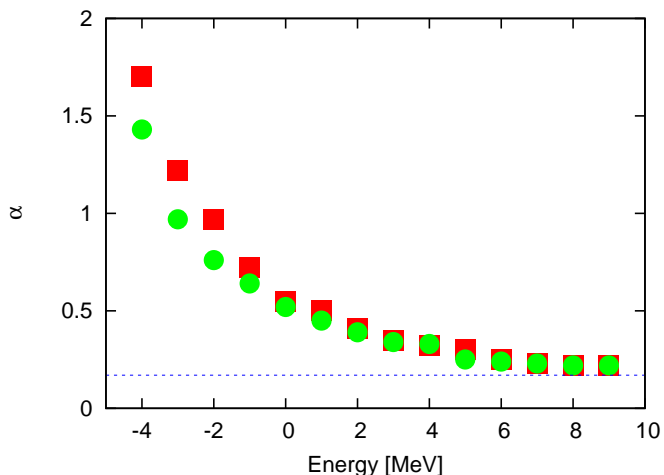
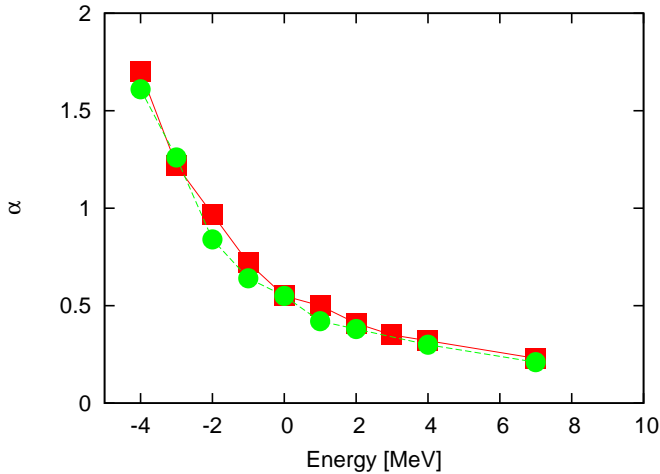


Fig. 4.  $\alpha$  as a function of energy for the two potential models at a fixed value of the density  $\rho = 0.007 \text{ fm}^{-3}$

It is clearly seen that for the high energy cases both curves converge to the same value and, consequently, the direct use of Eq. (2) does not seem to be correct.

### 3.3 Isoscaling for free expanding systems

We now try to explore if the problem found in the previous section remains when the systems are free to expand. For this purpose we take the configurations recorded for the confined equilibrated systems and we solve the equations of motion after removing the confining walls. By performing the same steps described above for the determination of the  $\alpha$  coefficient we obtain the results shown in Fig. 5.



**Fig. 5.**  $\alpha$  as a function of energy for the two potential models and  $\rho = 0.007 \text{ fm}^{-3}$

It can be seen that the overall picture remains the same so that the possibility of determining the symmetry energy term is once again blurred by the presence of the symmetry term.

## 4 Conclusions

We have calculated the isoscaling property using classical molecular dynamics simulations of confined and free to expand systems combined with a fragment-recognition algorithm. Systems with collisions of  $[Z = 40, N = 40]$  and  $[Z = 40, N = 56]$ , at total energies from  $-4$  to  $8 \text{ MeV/A}$  were used to construct the ratios  $R_{21}(N, Z)$  and to obtain the fitting parameters  $\alpha$  and  $\beta$ .

The fitting parameters of the  $R_{21}$  for the equilibrated systems showed a smooth variation with respect to the energy. Examining the energy evolution of the  $\alpha$  parameter we showed that it converges to the symmetric value. When the equilibrated system is left free to expand the same behavior is observed but the fitted values of the  $\alpha$  parameters are slightly below the confined ones.

Taking advantage of having two parameterizations of the systems we calculated the coefficients of the corresponding liquid drop expansion for the ground states energies. The convergence of the value of  $\alpha$  to the symmetric value does not allow to differentiate between the

two systems (characterized by the different sets of parameters of the interaction potential) at and above moderate values of the total energy.

In view of these findings we believe it is unlikely that the phenomenon of isoscaling is sensitive enough as to allow us extract detailed information about the symmetry energy term of the *EOS*.

## 5 Acknowledgments

C.O.D. is a member of the "Carrera del Investigador" CONICET. C.O.D. acknowledges the support of a grant from the Universidad de Buenos Aires, CONICET through grant PIP5969.

## References

1. H. S. Xu, M. B. Tsang, T. X. Liu, X. D. Liu, W. G. Lynch, W. P. Tan, A. Vander Molen, G. Verde, A. Wagner, H. F. Xi, C. K. Gelbke, L. Beaulieu, B. Davin, Y. Larochelle, T. Lefort, R. T. de Souza, R. Yanez, V. E. Viola, R. J. Charity and L. G. Sobotka, *Phys. Rev. Lett.* **85**, 716 (2000).
2. H. Johnston *et al.*, *Phys. Lett.* **B3715**, 186 (1996).
3. R. Laforest *et al.*, *Phys. Lett.* **C59**, 2567 (1999).
4. M. B. Tsang, C.K. Gelbke, X.D. Liu, W.G. Lynch, W.P. Tan, G. Verde, H.S. Xu, W. A. Friedman, R. Donangelo, S. R. Souza, C.B. Das, S. Das Gupta, D. Zhabinsky, *Study of isoscaling with statistical multifragmentation models*, *Phys. Rev.* **C64**, 054615 (2001).
5. M. B. Tsang, W. A. Friedman, C. K. Gelbke, W. G. Lynch, G. Verde and H. Xu, *Phys. Rev. Lett.* **86**, 5023 (2001).
6. C. B. Das, S. Das Gupta, X. D. Liu and M. B. Tsang, *Phys. Rev.*, **C64**, 044608 (2001)
7. A. Ono, P. Danielewicz, W. A. Friedman, W. G. Lynch, and M. B. Tsang, *Phys. Rev.* **C68**, 051601(R) (2003).
8. C. O. Dorso, C. R. Escudero, M. Ison and J. A. López, *Phys. Rev.* **C 73**, 044601 (2006).
9. A. Dávila, C. Escudero, J. A. López and C. O. Dorso, *Physica A* **374**, 663 (2007).
10. C. O. Dorso, *Phys. Rev.* **C73** 034605 (2006).
11. L. Moretto, C. O. Dorso, L. Phair and J.B.Elliott, *PPhys. Rev.* **C77** 037603 (2008).
12. R. J. Lenk, T. J. Schlagel and V. R. Pandharipande, *Phys. Rev.* **C42**, 372 (1990)
13. A. Chernomoretz, L. Gingras, Y. Larochelle, L. Beaulieu, R. Roy, C. St-Pierre and C. O. Dorso, *Phys. Rev.* **C65**, 054613 (2002).
14. A. Barrañón, C. O. Dorso and J. A. López, *Rev. Mex. Fís.* **47-Sup.2**, 93 (2001).
15. A. Barrañón, C. O. Dorso, and J. A. López, *Nuclear Phys.* **A791**, 222 (2007).
16. J.M. Rohlf, *Modern physics from a to Z*, John Wiley and Sons, (1994).
17. T.L. Hill, *J. Chem. Phys* **23**, 617 (1955).
18. A. Strachan and C. O. Dorso, *Phys. Rev.* **C56**, 995 (1997).
19. A. Chernomoretz, M. Ison, S. Ortiz and C.O.Dorso , *Phys. Rev.* **C64**, 024606 (2001).
20. M. J. Ison and C.O.Dorso , *Phys. Rev.* **C69**, 027001 (2004).